

Temperature- and injection-dependent lifetime spectroscopy for the characterization of defect centers in semiconductors

Jan Schmidt^{a)}

Institut für Solarenergieforschung Hameln/Emmerthal (ISFH), Am Ohrberg 1, D-31860 Emmerthal, Germany

(Received 11 December 2002; accepted 29 January 2003)

A highly sensitive, contactless defect characterization technique, temperature- and injection-dependent lifetime spectroscopy (TIDLS), is introduced. In this method, the injection-level-dependent carrier lifetime curves of a semiconductor are measured at various temperatures by means of an inductively coupled resonant circuit. In order to illustrate certain features of the TIDLS, the lifetime-limiting defect center in aluminum-doped Czochralski silicon is analyzed. It is shown that, compared to previous lifetime spectroscopy techniques, TIDLS not only determines the defect energy level with improved accuracy, but is also capable of determining the temperature dependence of the electron and hole capture cross sections. In addition, the method permits the separation between shallow and deep-level centers. © 2003 American Institute of Physics. [DOI: 10.1063/1.1563830]

Recombination lifetime spectroscopy is one of the most sensitive diagnostic tools for the identification and analysis of impurities in semiconductors. The principal advantage of lifetime spectroscopy over traditional defect characterization techniques such as deep-level transient spectroscopy¹ is that only those defect centers which contribute to the total recombination rate (that is, those centers that are actually relevant to semiconductor devices, like solar cells or random-access memories) are analyzed. In the past, energy levels and ratios of electron and hole capture cross sections have been determined for several well-defined impurities in silicon using temperature-dependent lifetime spectroscopy (TDLS).^{2–4} Standard TDLS measures the carrier lifetime of a sample under low-level injection conditions (τ^{LLI}) and determines the defect energy level E_t from the linear slope of the Arrhenius plot of $\ln(\tau^{LLI}/T)$ versus $1/T$.⁴ However, a basic assumption of the standard TDLS analysis is that the electron and hole capture cross sections σ_n and σ_p are independent of temperature, which is not valid in general. On the other hand, the evaluation of injection-dependent lifetime spectroscopy (IDLS) data usually results only in a relatively broad uncertainty range for E_t ,⁵ but is in most cases capable of determining the σ_n/σ_p ratio with high accuracy. In this letter, temperature- and injection-dependent lifetime spectroscopy (TIDLS) is introduced to combine the advantages of the two lifetime spectroscopy techniques just mentioned.

The contactless quasi-steady-state photoconductance (QSSPC) method developed by Sinton and Cuevas⁶ is used to measure the injection-level-dependent lifetime curves. A coil in a resonant circuit, operating at 13.56 MHz, couples to the conductivity of the sample. The output voltage of the bridge circuit is linear in wafer conductance over the entire measurement range. Reference wafers of known dark conductance are used to calibrate the rf bridge circuit. A conventional photo-flash light source, having a slow decay time of 1.8 ms, generates electron-hole pairs in the sample. As the

light pulse varies very slowly compared to the effective carrier lifetime of the sample, the latter is approximately under steady-state conditions during the complete 8-ms illumination time. The time-dependent light intensity, measured with a calibrated solar cell, as well as the rf bridge output voltage are recorded on a digital oscilloscope and transferred to a computer for analysis. From the measured photoconductance and light intensity data, the effective lifetime of the sample is calculated as a function of the injection density, as described in Ref. 7. One of the main advantages of the QSSPC technique over transient decay approaches is that the QSSPC allows the measurement of very low lifetimes over a broad injection range without fast electronics or short light pulses.⁶ In principle, it would also be conceivable to use a photoconductance decay technique to scan the injection level, and this would have the attractiveness of not having to model the temperature dependence of the mobilities (see below). However, the measurement range would be limited to relatively high lifetimes using the current apparatus.

In order to enable temperature-dependent measurements, the original QSSPC setup (Sinton Consulting Inc.) has been complemented with a temperature-controlled sample stage positioned on top of the photoconductance-sensor coil. The sample is placed on a PyrexTM glass disk kept at a distance of about 1 mm from the coil by means of insulating spacers. The wafer is brought in contact with a brass ring, which is heated using a resistive element. The temperature of the sample is measured with a thermocouple mounted on its surface and the heating power is regulated via a proportional controller. Although the heating stage is thermally insulated from the environment and the instrument, a slight heating of the coil cannot be completely avoided. Hence, we have measured the calibration curve of the rf bridge circuit at different temperatures of the reference wafers. Figure 1 shows the resulting calibration curves for temperatures ranging from 30 to 150 °C. The conductance of the reference wafers was calculated at the different temperatures using the majority carrier mobility parameterization of Ref. 8. The fact that the

^{a)}Electronic mail: j.schmidt@isfh.de

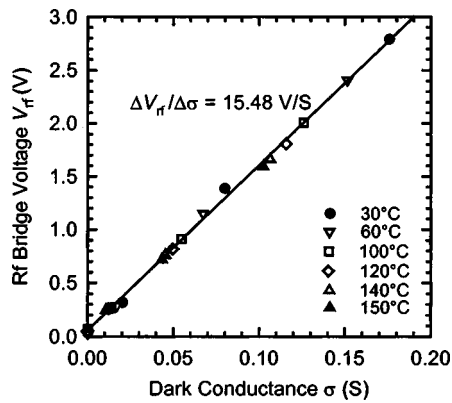


FIG. 1. Calibration curve of the rf bridge circuit measured at different temperatures of the reference wafers (30–150 °C). The dark conductance of the reference wafers depends strongly on temperature due to the temperature dependence of the majority carrier mobility.

slope of the calibration curve does not change with temperature shows that the small heating of the coil does not affect the lifetime measurements and that the setup is well suited for TIDLS applications.

For the determination of the carrier lifetime from the measured photoconductance data, it is very important to take the temperature dependence of the minority-carrier mobility into account. In this work, this was done using the empirical mobility parameterization of Arora *et al.*⁸ The small changes in the generation rate G can be neglected in the investigated temperature range (rising the temperature from 30 to 150 °C leads to an increase in G of only 4%). The total lifetime measurement error is estimated to be about 10%.

Recently, Rein *et al.*⁹ suggested the use of standard TDLS plus a single-temperature IDLS measurement to determine defect parameters with improved accuracy. In the TIDLS method we go one step further by measuring many IDLS curves at various temperatures. The increased information on the two dependencies of the lifetime decreases the uncertainty of the theoretical analysis and enhances its capabilities. As a third parameter, it would also be possible to vary the wafer doping level, which in combination with IDLS can also provide sufficient information.⁵ However, the latter approach has many practical disadvantages, including the possible change of the nature of the recombination center due to interactions with the dopant atoms.

The application of the TIDLS is demonstrated on an Al-doped Czochralski (CZ) silicon wafer with a resistivity of 2.0 Ωcm (doping concentration $7.2 \times 10^{15}\text{ cm}^{-3}$). The lifetime in this material is known to be dominated by a characteristic Al-related defect species.² In order to remove other metallic impurities from the material, a phosphorous gettering treatment has been applied.¹⁰ After removing the phosphorous-doped surface layer using acidic etching and RCA cleaning of the wafer, 80-nm-thick silicon nitride layers have been deposited onto both surfaces by plasma-enhanced chemical vapor deposition.¹¹ Due to the excellent surface passivation quality of these silicon nitride films,¹¹ recombination in the sample is virtually completely restricted to the silicon bulk.

Following the standard TDLS analysis, we first only evaluate the low-level injection lifetime $\tau_{\text{eff}}^{\text{LLI}}$ measured at a fixed injection density of $\Delta n = 1 \times 10^{14}\text{ cm}^{-3}$ (for $\Delta n \leq 1$

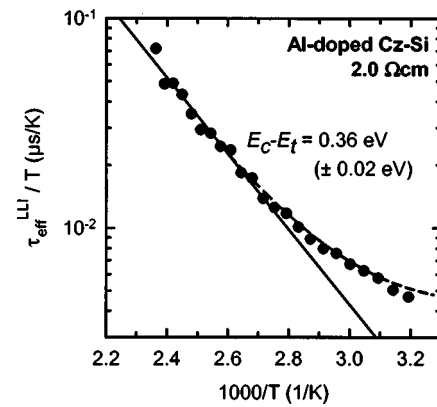


FIG. 2. Standard TDLS analysis of the low-level injection lifetime $\tau_{\text{eff}}^{\text{LLI}}$ as a function of inverse temperature $1000/T$ of an Al-doped CZ-Si sample.

$\times 10^{14}\text{ cm}^{-3}$, trapping effects may hamper the lifetime measurements) for temperatures between 30 and 150 °C. Figure 2 shows the corresponding Arrhenius plot of $\tau_{\text{eff}}^{\text{LLI}}/T$ versus $1000/T$. The data points measured at temperatures above 90 °C are on a straight line. The slope of the linear fit (solid line) gives an energy level of $0.36 \pm 0.02\text{ eV}$ for the lifetime-limiting defect. However, the linear part of the curve does not reveal if the energy level lies in the upper or lower half of the band gap. Only a fit over the entire temperature range using the complete Shockley-Read-Hall (SRH) equation^{12,13} (dashed line) shows that the energy level lies in the upper half of the band gap at $E_c - E_t = 0.36\text{ eV}$.

If this were the true energy level of the defect, it should be possible to fit the complete set of injection-dependent lifetime curves measured at temperatures ranging from 30 to 150 °C. However, it turns out that this is not possible with the energy level determined from the standard TDLS analysis. In fact, the energy level has to lie much deeper in the band gap at $E_c - E_t = 0.45\text{--}0.90\text{ eV}$ to allow a simultaneous fit of all injection- and temperature-dependent lifetime curves. The broadness of the E_t range obtained from the TIDLS analysis is a consequence of the fact that all energy levels within this range have virtually the same recombination strength, so that the uncertainty does not matter in practice. An additional recombination center with a shallow energy level at 0.14 eV below E_c or above E_v is required to obtain a good fit over the entire injection range. Figure 3 shows the measured TIDLS curves together with the corresponding SRH fits, including the deep and the shallow defect levels. In the literature, two dominant bulk defect levels at $E_c - E_t = 0.80\text{ eV}$ and $E_t - E_v = 0.22\text{ eV}$ have been identified in Al-doped CZ-Si using DLTS.¹⁴ Both defects were assigned to aluminum-oxygen complexes. The DLTS energy levels are in satisfactory agreement with the deep and the shallow defect levels determined from our TIDLS analysis. We have not observed any changes in the lifetime, and hence in the defect concentration, due to annealing or illumination of the Al-doped CZ-Si samples.

Another important defect parameter that can be extracted from the TIDLS analysis is the temperature-dependent ratio of the capture cross sections σ_n/σ_p , which is assumed to be temperature-independent in the standard TDLS analysis. The experimentally accessible parameters are the capture-time constants for electrons $\tau_{n0} = (N_t \sigma_n \nu_{\text{th}})^{-1}$ and holes τ_{p0}

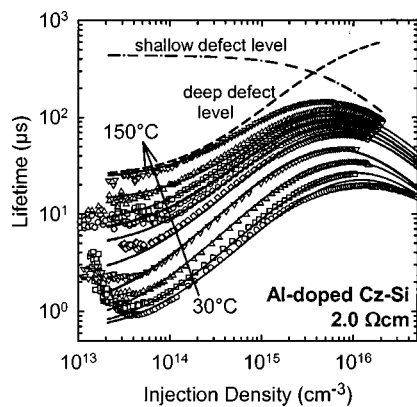


FIG. 3. Measured injection dependence of the effective carrier lifetime at sample temperatures ranging from 30 to 150 °C (symbols) for the same sample as in Fig. 2. The lines show the SRH fits to the TIDLS curves including a deep and a shallow defect center. The SRH lifetimes of the deep (dashed line) and the shallow center (dash-dotted line) are separately shown at 150 °C.

$=(N_t \sigma_p \nu_{th})^{-1}$, where ν_{th} is the average thermal velocity of the free carriers and N_t is the defect concentration. While the temperature-dependent ν_{th} is well known,¹⁵ it is generally not possible to separate the capture cross section from the defect concentration using lifetime spectroscopic methods. However, the ratio of the microscopic electron and hole capture cross sections can be easily determined via $\sigma_n/\sigma_p = \tau_{p0}/\tau_{n0}$. The SRH fits shown in Fig. 3 force a very strong temperature dependence of σ_n/σ_p due to the temperature-dependent hole capture cross section σ_p (σ_n is temperature independent within the accuracy of the measurement). σ_n/σ_p increases from approximately 90 at 30 °C to about 1300 at 150 °C. Figure 4 shows the product of σ_p and the defect concentration N_t of the deep-level center as a function

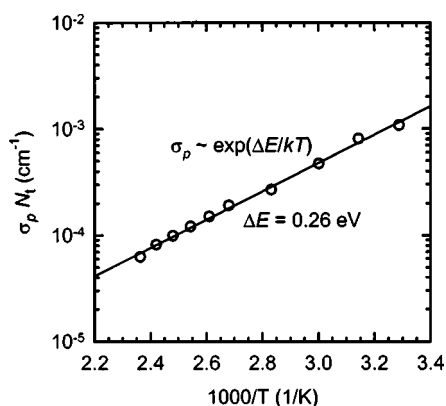


FIG. 4. Temperature dependence of the hole capture cross section σ_p times the concentration N_t of the deep-level center in Al-doped CZ-Si as determined from the TIDLS analysis (open circles). The solid line is an exponential fit to the measured data.

of the inverse temperature. The measured data can be fitted using an exponential dependence $\sigma_p \sim \exp(\Delta E/kT)$, with $\Delta E = 0.26$ eV. Such a strong temperature dependence of a capture cross section may be explained via a cascade capture at high temperature.^{16,17}

In conclusion, temperature- and injection-dependent lifetime spectroscopy has been shown to be a simple yet effective tool for the analysis of defect properties in semiconductors. The method is based on contactless measurements of the recombination lifetime of a semiconductor as a function of the excess carrier concentration at various temperatures. A simultaneous fit to all measured TIDLS curves using the Shockley–Read–Hall equation gives the defect energy level and the temperature dependence of the electron and hole capture cross sections. Furthermore, deep and shallow defect levels can be separated by this method. Standard low-level injection TDLS assumes temperature-independent capture cross section and measures only deep defect levels. However, as temperature-dependent capture cross sections are the rule rather than the exception, the standard TDLS analysis may lead in most cases to erroneous defect energy levels. Hence, compared to previous lifetime spectroscopy methods, the advanced TIDLS technique gives a considerably improved accuracy in the determination of defect properties.

The author would like to thank R. Sinton (Sinton Consulting Inc.) for technical assistance and fruitful discussions, and R. Hezel (ISFH) for his continuous support. Funding was provided by the State of Lower Saxony. The ISFH is a member of the German *Forschungsverbund Sonnenenergie*.

¹D. V. Lang, J. Appl. Phys. **45**, 3023 (1974).

²F. Shimura, T. Okui, and T. Kusama, J. Appl. Phys. **67**, 7168 (1990).

³Y. Kirino, A. Buczkowski, Z. J. Radzinski, G. A. Rozgonyi, and F. Shimura, Appl. Phys. Lett. **57**, 2832 (1990).

⁴S. Rein, T. Rehrl, W. Warta, and S. W. Glunz, J. Appl. Phys. **91**, 2059 (2002).

⁵J. Schmidt and A. Cuevas, J. Appl. Phys. **86**, 3175 (1999).

⁶R. A. Sinton and A. Cuevas, Appl. Phys. Lett. **69**, 2510 (1996).

⁷H. Nagel, C. Berge, and A. G. Aberle, J. Appl. Phys. **86**, 6212 (1999).

⁸N. D. Arora, J. R. Hauser, and D. J. Roulston, IEEE Trans. Electron Devices **29**, 292 (1982).

⁹S. Rein, P. Lichtner, W. Warta, and S. W. Glunz, *Proceedings of the 29th IEEE Photovoltaic Specialists Conference, New Orleans, LA* (IEEE, New York, 2002), p. 190.

¹⁰H. Nagel, J. Schmidt, A. G. Aberle, and R. Hezel, *Proceedings of the 14th European Photovoltaic Solar Energy Conference, Barcelona, Spain* (Stephens, Bedford, 1997), p. 762.

¹¹T. Lauinger, J. Schmidt, A. G. Aberle, and R. Hezel, Appl. Phys. Lett. **68**, 1232 (1996).

¹²W. Shockley and W. T. Read, Phys. Rev. **87**, 835 (1952).

¹³R. N. Hall, Phys. Rev. **87**, 387 (1952).

¹⁴R. L. Marchand and C. T. Sah, J. Appl. Phys. **48**, 336 (1977).

¹⁵M. Green, J. Appl. Phys. **67**, 2944 (1990).

¹⁶R. M. Gibb, G. J. Rees, B. W. Thomas, B. L. H. Wilson, B. Hamilton, D. R. Wight, and N. F. Mott, Philos. Mag. **36**, 1021 (1977).

¹⁷H. G. Grimmeiss and E. Janzén, in *Deep Centers in Semiconductors*, 2nd ed., edited by S. T. Pantelides (Gordon and Breach Science, Yverdon, Switzerland, 1992), p. 87.